

Jaws-only IMRT using direct aperture optimization

M. A. Earl,^{a)} M. K. N. Afghan, C. X. Yu, Z. Jiang, and D. M. Shepard

University of Maryland School of Medicine, Department of Radiation Oncology, 22 South Greene St., Baltimore, Maryland 21201-1595

(Received 26 June 2006; revised 6 November 2006; accepted for publication 6 November 2006; published 26 December 2006)

Using direct aperture optimization, we have developed an inverse planning approach that is capable of producing efficient intensity modulated radiotherapy (IMRT) treatment plans that can be delivered without a multileaf collimator. This “jaws-only” approach to IMRT uses a series of rectangular field shapes to achieve a high degree of intensity modulation from each beam direction. Direct aperture optimization is used to directly optimize the jaw positions and the relative weights assigned to each aperture. Because the constraints imposed by the jaws are incorporated into the optimization, the need for leaf sequencing is eliminated. Results are shown for five patient cases covering three treatment sites: pancreas, breast, and prostate. For these cases, between 15 and 20 jaws-only apertures were required per beam direction in order to obtain conformal IMRT treatment plans. Each plan was delivered to a phantom, and absolute and relative dose measurements were recorded. The typical treatment time to deliver these plans was 18 min. The jaws-only approach provides an additional IMRT delivery option for clinics without a multileaf collimator. © 2007 American Association of Physicists in Medicine. [DOI: [10.1118/1.2403966](https://doi.org/10.1118/1.2403966)]

Key words: IMRT, direct aperture optimization, jaws-only IMRT, inverse treatment planning

I. INTRODUCTION

Intensity modulated radiotherapy (IMRT) is an increasingly common clinical delivery technique. The widespread adoption of IMRT has been made possible by the availability of multileaf collimators (MLCs) that are capable of generating complex fluence maps by overlapping multiple fields from a single beam angle. Clinical implementation of IMRT is considerably more complicated for facilities without a multileaf collimator. For these clinics, IMRT has only been possible through the use of compensators. Compensators provide a relatively low-tech approach for producing IMRT treatment plans.¹⁻³ There are, however, a number of disadvantages to the use of compensators including: (1) the production of compensators is labor intensive and time consuming; (2) the therapists must enter the treatment room between each field in order to change to the next compensator; (3) it is difficult to achieve high spatial variation of intensities with compensators; (4) compensators are a major source of unwanted scatter; (5) scattered photons and beam hardening effects must be accounted for in order to make accurate dose calculations; and (6) a large amount of storage space is required if a clinic wishes to treat a large number of IMRT patients with compensators.

These issues have led investigators to explore the feasibility of delivering IMRT using a jaws-only approach.⁴⁻⁷ With this technique, multiple rectangular fields are delivered from each beam direction to create complex intensity patterns. One approach to developing jaws-only plans is to utilize a leaf sequencer modified to produce only rectangular fields. Leaf sequencers are used as part of a two-step approach to generating IMRT plans. First, the relative weights of a set of pencil beams are optimized for each beam angle. During the optimization, the delivery constraints are ignored.

The resulting intensity maps are then converted into a set of deliverable aperture shapes. The delivery constraints are enforced in this second “leaf-sequencing” step.

Dai and Hu⁴ demonstrated the feasibility of a jaws-only leaf sequencer that was designed to only produce rectangular fields. Depending on the complexity of the optimized intensity maps, their results demonstrated that between 4 and 10 times as many segments were required to replicate the fluence maps as compared with delivery using a multileaf collimator. A critical consequence of this increased number of segments is the corresponding lengthening of the delivery time by a factor of 2–5. These prolonged treatment times limit the clinical usefulness of this approach.

Webb⁵⁻⁷ proposed a more sophisticated technique where a special device could be used in conjunction with a jaws-only delivery approach to generate variable intensity patterns. The device is essentially a binary collimator where the apertures are the size of a beamlet and are either open or closed.

In this work, we have studied the ability of direct aperture optimization (DAO) to generate efficient jaws-only IMRT plans. DAO is an IMRT optimization technique that directly optimizes the aperture shapes and their corresponding weights thereby eliminating the need for a leaf-sequencing step. Any delivery constraints are enforced during the optimization. This feature allows us to generate IMRT treatment plans for linear accelerators without a MLC. For MLC-based DAO (MLCDAO), the variables that are optimized are the leaf positions and weights of the apertures in the plan. For “jaws-only” DAO (JODAO) described in this paper, the variables that are optimized are the jaw positions and weights of the apertures.

To illustrate the feasibility of the JODAO scenario, we selected five clinical patient cases to which we applied this

technique: two pancreas, a breast, and two prostate. For each case, we compared the results of JODAO to that of ML-CDAO. We also examined how many segments are required for the JODAO case to achieve a treatment plan that is comparable to that obtained with the MLCDAO case. In general, we found that 15–20 jaws-only segments were required to produce high-quality IMRT treatment plans.

II. MATERIALS AND METHODS

DAO is an inverse planning technique whereby the aperture shapes and relative weights of the segments are simultaneously optimized. This is in contrast to the traditional approach that employs two distinct steps: optimization and leaf sequencing. DAO results in a deliverable treatment plan immediately after optimization; no further leaf sequencing is needed. We have presented the technique in detail in previous works^{8,9} so only a brief overview is provided here.

Generating DAO plans is accomplished via the following sequence: (1) the delivery angles and isocenter are specified along with the number of apertures from each angle; (2) the patient-specific pencil beam dose distributions are computed; (3) the treatment goals are defined and translated into an objective function; (4) the optimization is performed with a simulated annealing algorithm; and (5) the final plan is output for analysis, delivery, verification, and treatment.

In some linear accelerator designs, one set of jaws cannot cross the central axis. This can impact the appropriate selection of the isocenter for JODAO planning. However, for all cases in this study, the isocenter was placed in the geometric center of the target volume and jaw over-travel was not problematic.

After the user decides upon the appropriate delivery angles and isocenter, patient-specific pencil beam dose distributions are computed. The Prowess planning system utilizes a convolution based dose calculation. Because the jaw movement is continuous, the pencil beams can be any size. However, for the cases presented in this paper, we used a pencil beam size of 1 cm × 0.5 cm projected to isocenter. This made it possible to use the same pencil beams for the JODAO and the MLCDAO plans. We should note that for the Elekta machines in our clinic (using the IEC 1217 convention), this pencil beam size allows the *X* jaws to move in 0.5 cm increments and the *Y* jaws to move in 1 cm increments.

After the pencil beams were calculated, the user defines the clinical objectives. The objective function used in this study is based on a least-squares penalty of the form:

$$O = w \times (d_p - d_i)^2, \quad (1)$$

where w is an importance weighting, d_p is the prescription dose for the volume, and d_i is the dose to the i^{th} voxel. This simple least-squares form of objective function allows for minimum dose, maximum dose, and dose volume histogram objectives. For instance, a maximum dose objective penalizes points within the volume of interest that are above d_p by $w \times (d_p - d_i)^2$.

The optimization is performed using simulated annealing.¹⁰ At each iteration of the optimization, a parameter is randomly selected. For example, in the case of JODAO, the parameters are jaw positions and weights of the apertures. After the selection of the parameter, a change is sampled from a Gaussian distribution. The width of the Gaussian decreases according to the schedule

$$\sigma = 1 + (A - 1) \times e^{-n_{\text{succ}}/T_0^{\text{step}}}, \quad (2)$$

where A is the width of the Gaussian at the beginning of the optimization, n_{succ} is the number of successes (defined below), and T_0^{step} dictates the rate at which the width of the Gaussian decreases. As $n_{\text{succ}} \rightarrow \infty$, $\sigma \rightarrow 1$, avoiding changes that are zero.

After each change in jaw position, the new aperture is checked to determine if it satisfies the delivery constraints. For the cases in this paper, we enforce a constraint that one set of jaws cannot travel across the central axis, as is the case with the Elekta accelerators at our institution. Another constraint that we enforce is that the jaws must be separated by at least 1 cm. To avoid apertures that are too small, we also enforce a constraint that the equivalent square of the aperture must be greater than 3.0 cm. If the change does not satisfy the delivery constraints, it is discarded and a new parameter is selected and changed.

If the change satisfies the delivery constraints, the dose for the new aperture is computed by adding or subtracting the dose contributions of the relevant pencil beams from the current dose distribution. The objective function value is then calculated based on the new dose distribution. If the objective function value is reduced (plan improvement), the change is automatically accepted. If the objective function value becomes larger (plan degradation), the new change is accepted with a probability p given by

$$p = B \frac{1}{(n_{\text{succ}} + 1)^{1/T_0^{\text{prob}}}}, \quad (3)$$

where B is the probability at the start of the optimization, n_{succ} is the number of successes, and T_0^{prob} dictates the rate at which this probability decreases. As $n_{\text{succ}} \rightarrow \infty$, $p \rightarrow 0$. Thus as the optimization progresses, the algorithm is less and less likely to accept a change that reduces the plan quality. The purpose of accepting changes that result in a degradation in the plan quality is to avoid becoming trapped in local minima. A success is defined as a change that either results in a lower objective function value or a change that results in a higher objective function value but passes the probability constraint.

Our direct aperture optimization (DAO) technique has been incorporated into the Prowess treatment planning system (Prowess Inc., Chico, CA). Prowess is capable of producing both MLCDAO and JODAO plans. All cases presented in this work were planned using the Prowess system that runs on a stand-alone PC running Windows XP. For each case, multiple optimizations were run using JODAO varying the number of apertures per beam. In addition, an MLCDAO plan was created using the same treatment objectives.

For each case, a MLCDAO and a JODAO plan were transferred to the RTDesktop (version 4.2) control system of an Elekta Precise linear accelerator. The plans were then delivered to a cylindrical phantom where an absolute measurement was performed with an ionization chamber. The relative dose was measured with Kodak EDR2 film. The film was placed in the transverse plane at the isocenter. The agreement between predicted and measured results was evaluated and the treatment times were compared for JODAO and MLCDAO, where treatment time is defined as the difference between the “beam-on” time for the first field and the “beam-off” time for the last field. Treatment time therefore includes any time required for the control computer to load the beam and any time taken to move from one field to the next.

III. RESULTS

A. Pancreas 1

For this case, seven approximately equispaced beams were used. The starting field sizes were set to 14×16 , thus 3136 ($7 \times 14 \times 16 \times 2$) pencil beams were computed. The dose computation took approximately 2.5 h. JODAO optimizations were performed with 5, 10, 15, 20, and 25 apertures per beam and compared with the result from the benchmark MLCDAO case which used seven apertures per beam direction. Each optimization took approximately 2.5 h to run with 10 000 optimization iterations. For all the optimizations, plan improvement was minimal after around 9000 iterations.

The gross tumor volume (GTV) was in the abdominal region in close proximity to both kidneys. The prescribed target dose for this case was 180 cGy for 28 fractions. The right kidney was closer to the GTV, so the primary goal was to keep as much of the left kidney as possible below tolerance dose of 2000 cGy (between 70 and 75 cGy per fraction). Per fraction, the secondary clinical goals were to keep the dose to the right kidney sufficiently low, keep the cord dose below 150 cGy, and to ensure that the planning target volume (PTV) was covered by 170 cGy (95% of the prescription dose).

Figure 1 shows the final objective function value as a function of the number of apertures used. When 15 jaws-only apertures were used per beam direction, the JODAO plan provided an objective function value that was nearly identical to that achieved with MLCDAO. Note that beyond 15 jaws-only apertures per angle, slight increases in the objective function value were observed. This may indicate that the optimizer failed to reach global optimality due to a lack of sufficient iterations or a cooling scheme for the simulated annealing that was not sufficiently slow. Figure 2 provides dose volume histogram (DVH) comparisons between the MLCDAO and JODAO (15 aps) plans. Similar target coverage and sparing of the both kidneys were observed for the two plans. The jaws-only plan led to an increase in the mean dose to the left kidney from 47% to 52% of the prescribed dose. Figure 3 shows an isodose distribution comparison for the two plans.

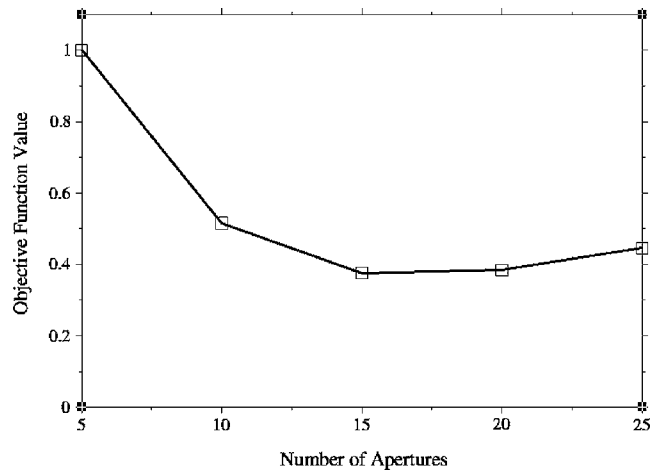


FIG. 1. Final objective function value is plotted as a function of the number of apertures the JODAO plans for the first pancreas case. For reference, MLCDAO plan that utilized seven apertures per beam direction had a final objective function value of 0.394.

After optimization, the treatment parameters for the JODAO (15 aps) case were transferred to the control computer of our Elekta Precise linear accelerator. We then delivered the plan to the cylindrical phantom and measured absolute dose with an ionization chamber and relative dose using Kodak EDR2 film. The absolute dose measurement was 2.3% from that predicted by the calculation. A gamma analysis was performed on the film measurement and 89% of the pixels passed the criteria of 3%/3 mm dose and distance agreement. The delivery time for this plan was 16 min. For comparison, the JODAO (15 aps) plan required 1161 MUs while the MLCDAO required 538 MUs.

B. Breast carcinoma

This case was used to test the capabilities of JODAO for tangential breast irradiation. First, a MLCDAO treatment plan was developed using five apertures per beam angle.

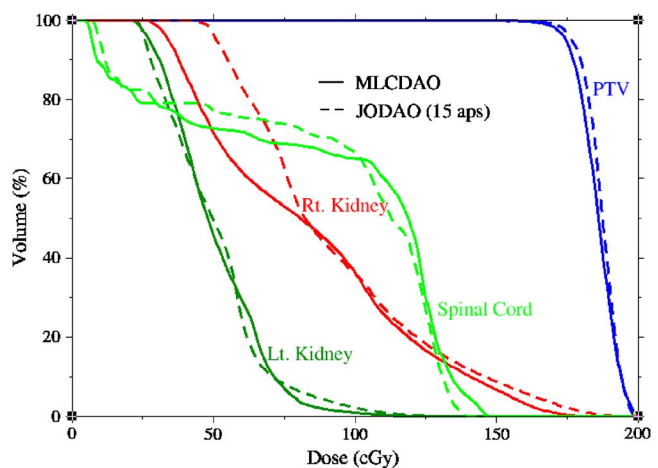
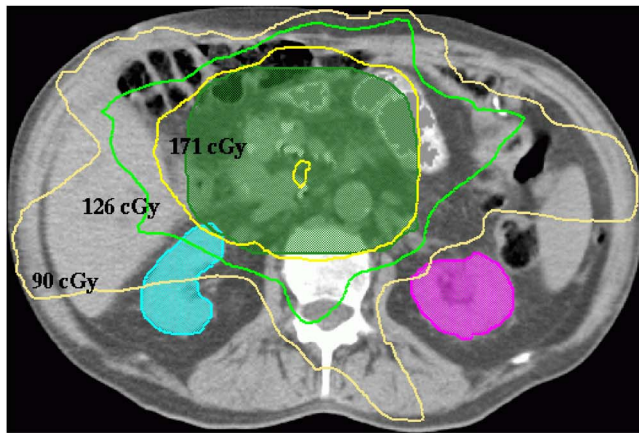
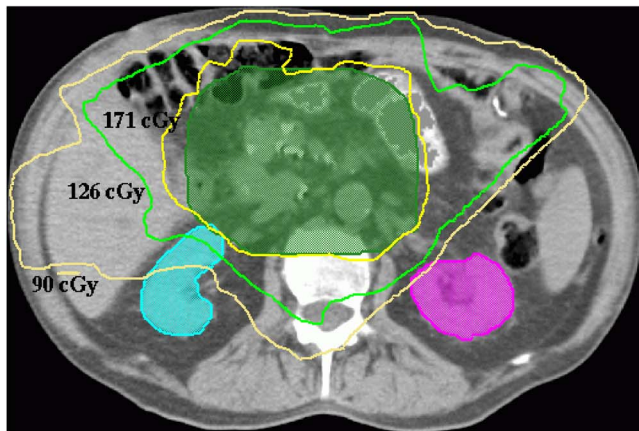


FIG. 2. Dose volume histogram for the pancreas 1 patient. Solid lines denote the MLCDAO plan with seven apertures per beam angle, whereas the dashed lines denote JODAO plan with 15 apertures per beam angle.



(a)



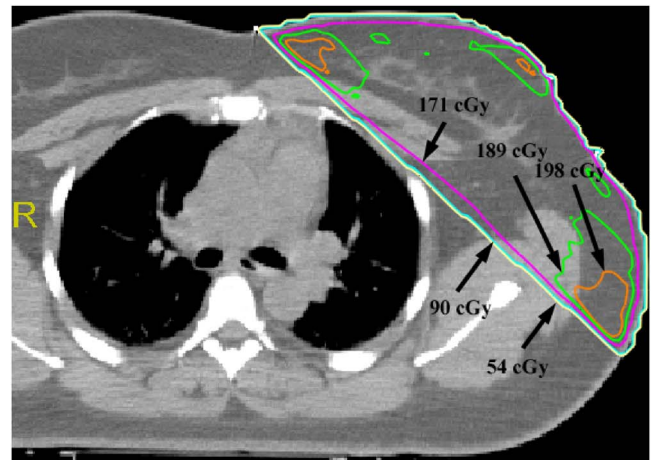
(b)

FIG. 3. Comparison of isodose distributions between MLCDAO (a) and JODOA (b) plans for the pancreas 1 patient. The 171, 126, and 90 cGy lines are shown (corresponding to the single fraction prescription dose of 90%, 70%, and 50%).

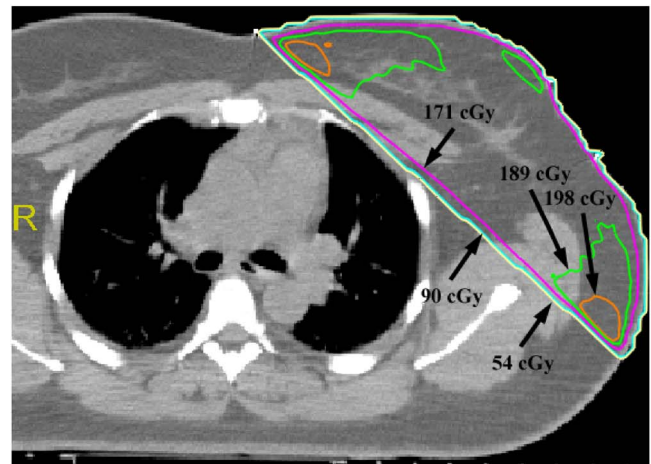
Next, a JODOA treatment plan was created using 15 apertures per beam direction. The same treatment objectives were used for each optimization. Figure 4 shows the comparison of isodose distribution for the two plans. The 198, 189, 171, 90, and 54 cGy isodose lines are shown (corresponding to 110%, 105%, 95%, 50% and 30% of the single fraction prescription). Figure 5 plots the DVH comparison. It can be seen that the jaws-only approach provided similar plan quality as achieved using MLC-based IMRT. Each plan was delivered to the cylindrical phantom. This plan was delivered in approximately 5 min on an Elekta SL18 linear accelerator. The absolute dose measurement was 3.0% from that predicted by the calculation. The JODOA plan required 259 MU while the MLCDAO plan required 254 MU.

C. Prostate patient 1

The MLCDAO plan for this prostate patient used seven beam angles with five apertures per beam angle. The JODOA (15 aps) plan used the same beam arrangement with 15 apertures per angle. The prescription parameters were kept the same for both the plans. A comparison of isodose distributions is provided in Fig. 6. A DVH comparison is shown in



(a)



(b)

FIG. 4. Comparison of isodose distributions between MLCDAO (a) and JODOA (15 aps) (b) plans for the breast carcinoma. The 198, 189, 171, 90, and 54 cGy lines are shown (corresponding to 110%, 105%, 95%, 50% and 30% of the single fraction prescription dose of 180 cGy). Note similar high dose gradients in both the cases but slightly increased hot spots in the MLCDAO plan.

Fig. 7. Very similar PTV coverage was achieved by both plans. However, with the JODOA (15 aps) plan, the mean dose to the bladder increased from 97.8 to 107.2 cGy. The mean dose to the rectum increased from 114.5 to 122.2 cGy. The plan was delivered in approximately 21 min on an Elekta SL18 linear accelerator and had an absolute dose difference of 4.5% from that predicted by the calculation. The JODOA plan required 411 MU while the MLCDAO plan required 425 MU.

D. Prostate patient 2

The MLCDAO benchmark plan was created using seven beam angles with five apertures per beam. The JODOA plan used identical beam angles with 20 apertures per beam angle, however, two collimator angles were used for each beam angle: 0 and 45°. The use of multiple collimator angles provides an improved ability to achieve complex intensity maps when restricted to rectangular field shapes. The same treatment objectives were used in both optimizations. Figure 8

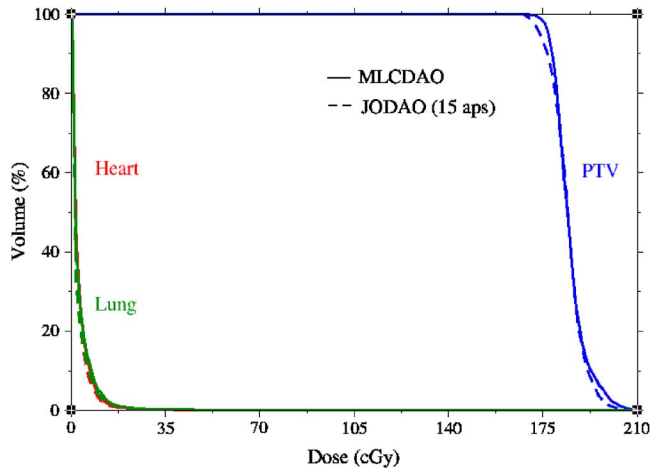


FIG. 5. Dose volume histogram for the breast carcinoma case. Solid lines denote the MLCDAO plan with five apertures per beam angle whereas the dashed lines denote JODAO (15 aps) plan.

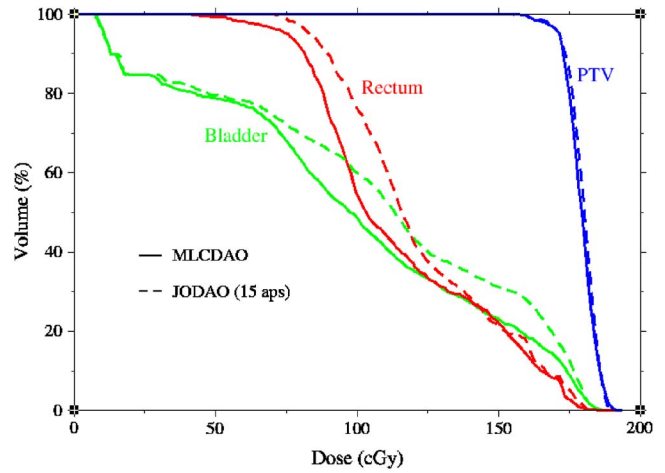
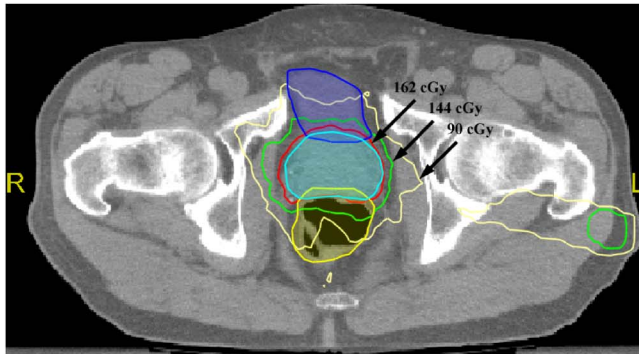


FIG. 7. Dose volume histogram for prostate patient 1. Solid lines denote the MLCDAO plan with five apertures per beam angle, whereas the dashed lines denote JODAO (15 aps) plan.

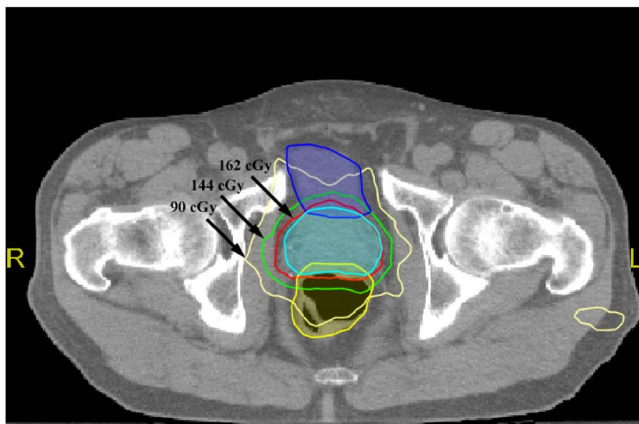
shows a comparison of the isodose distributions on axial view. Figure 9 shows the same comparison on coronal and sagittal views.

In Fig. 10, DVHs are shown for the MLCDAO and JODAO (20 aps) plans. Note that both of the plans provide

similar target coverage. In the low dose region, MLCDAO is better at sparing bladder but in the high dose region both the plans are very similar. The JODAO (20 aps) plan provides improved sparing of the rectum in the low and high dose

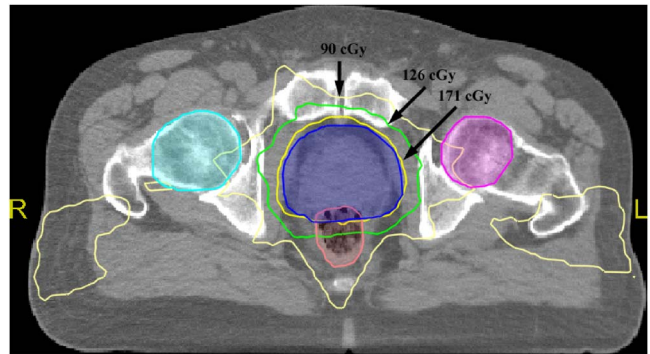


(a)

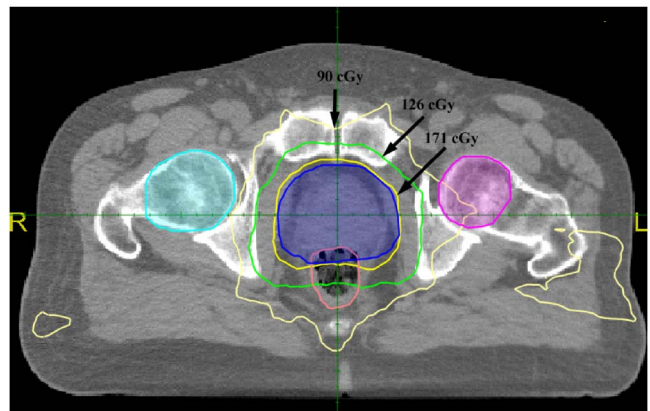


(b)

FIG. 6. Comparison of isodose distribution between MLCDAO (a) and JODAO (15 aps) (b) plans for the prostate patient 1. The PTV, bladder, and rectum are shown. Isodose lines shown are 162, 144, and 90 cGy (corresponding to 90%, 80% and 50% of the single fraction prescription dose of 180 cGy).



(a)



(b)

FIG. 8. Comparison of isodose distribution between the MLCDAO (a) and JODAO (20 aps) (b) plans for the prostate patient 2. Isodose lines shown are 171, 126, and 90 cGy (corresponding to 95%, 70% and 50% of the single fraction prescription dose of 180 cGy).

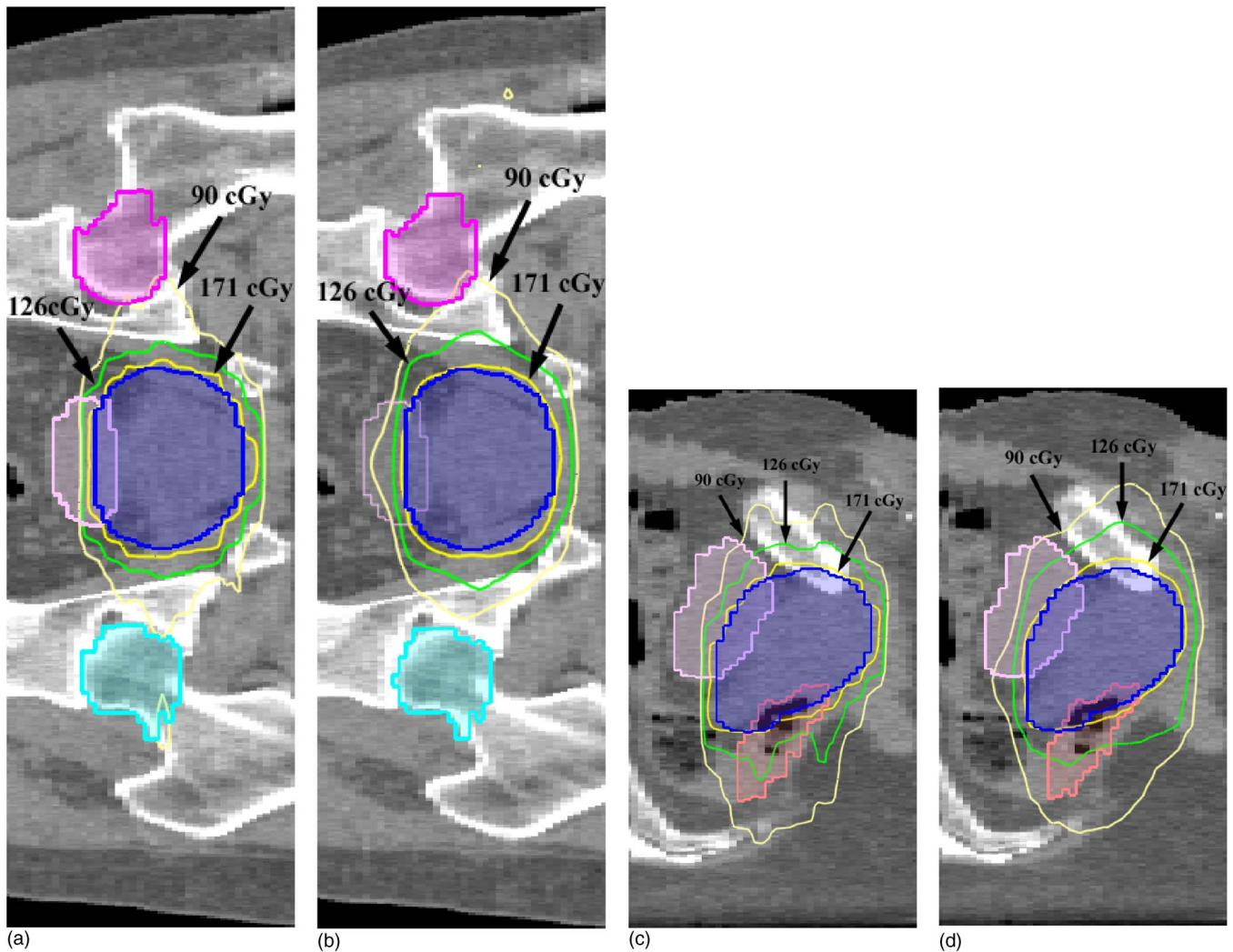


FIG. 9. Comparison of isodose distribution on coronal and sagittal sections between the MLCDAO and JODAO (20 aps) plans for prostate patient 2. Isodose lines shown are 171, 126, and 90 cGy (corresponding to 95%, 70% and 50% of the single fraction prescription dose of 180 cGy). (a) A coronal section from the MLCDAO plan. (b) Same slice from the JODAO (20 aps) plan. (c) A sagittal section from the MLCDAO plan. (d) Same slice from the JODAO (20 aps) plan.

regions. Although the MLCDAO plan shows better sparing of left femoral head, the JODAO (20 aps) plan provides better sparing of right femoral head.

Figure 11 shows the isodose comparison between the film measurement and the dose calculation. The 90%, 70%, and 50% isodose lines are shown and the agreement satisfies our IMRT verification criteria. The absolute dose measurement was 3.1% different from that predicted by Pinnacle³. The plan was delivered in approximately 34 min on an Elekta SL18 linear accelerator. The delivery time for this plan is longer compared with the other plans in this study. The reason for this was that two collimator angles were used from each beam direction. The control computer of the linac must therefore load two beams for each gantry angle. The additional loading time contributes a considerable amount of time to the total delivery time. The JODAO required 377 MU while the MLCDAO plan required 375 MU.

We should note here that future work in the area of jaws only IMRT could include an investigation into the ability to

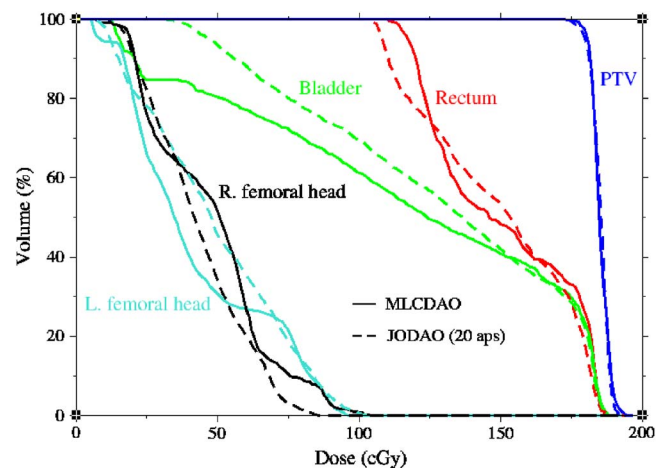


FIG. 10. Dose volume histogram for the prostate patient 2. Solid lines denote MLCDAO plan with five apertures per beam angle, whereas dashed lines denote JODAO (20 aps) plan.

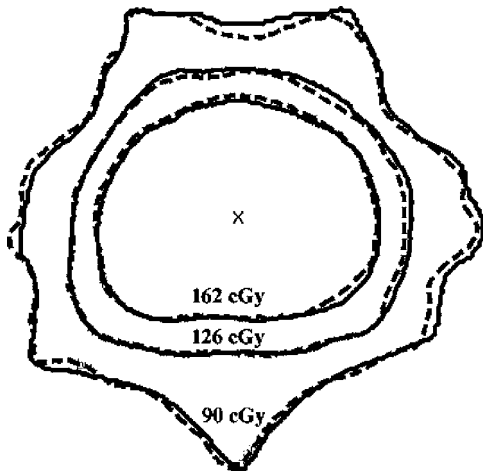


FIG. 11. Isodose overlay for the verification of prostate patient 2. Solid lines represent calculated dose and dashed lines denote delivered dose. Isodose lines shown are 162, 126, and 90 cGy (corresponding to 90%, 70%, and 50% of the prescription dose of 180 cGy). The point of absolute dose measurement is denoted with an *x*.

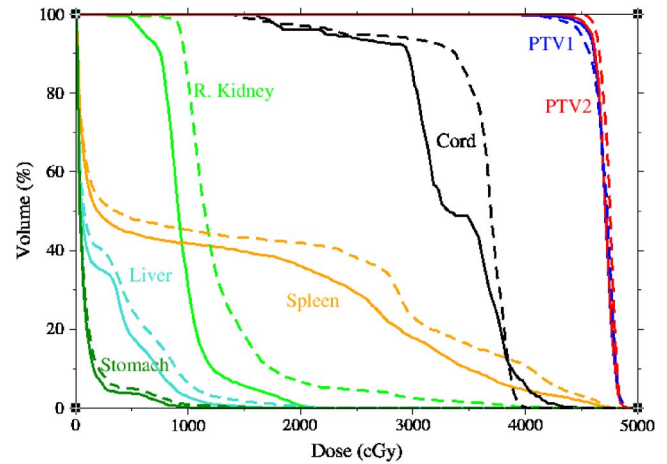
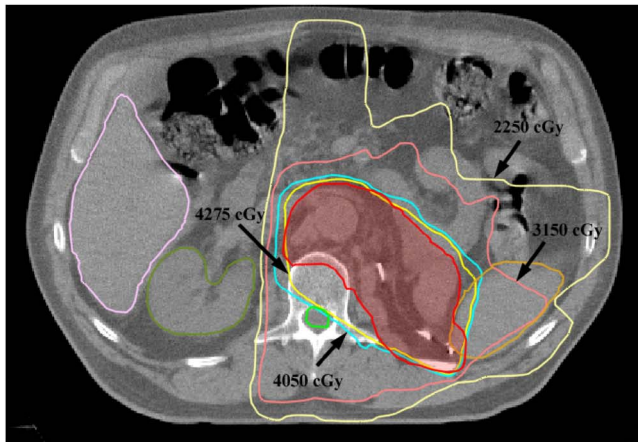
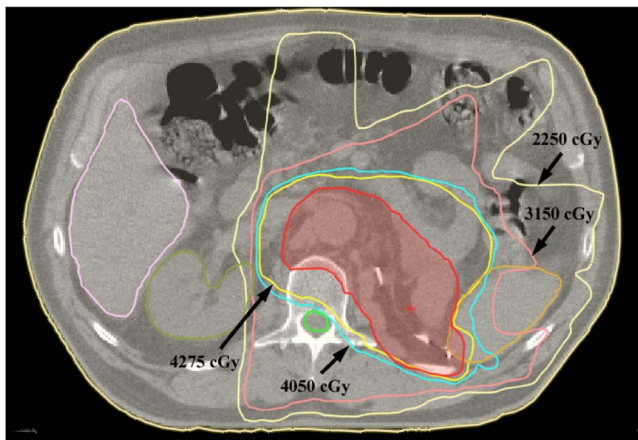


FIG. 13. Dose volume histogram for the pancreas patient. Solid lines denote MLCDAO plan with five apertures per beam angle, whereas dashed lines denote JODAO (15 aps) plan.



(a)



(b)

FIG. 12. Comparison of isodose distribution between the MLCDAO (a) and JODAO (15 aps) (b) plans for the pancreas patient. The 4275, 4050, 3150, and 2250 cGy isodose lines are shown (corresponding to 95%, 90%, 70%, and 50% of the total prescription dose of 4500 cGy).

improve plan quality by incorporating the collimator angle as a variable in the optimization. Optimization of the collimator angles would dramatically increase both the amount of data and the complexity of the optimization and is therefore beyond the scope of this work.

E. Pancreas

Two treatment plans, with five beams each, were optimized using the same beam arrangement and dose constraints. For the MLCDAO plan, five apertures per beam angle were used. The JODAO plan used 15 apertures per beam angle. A comparison of isodose distributions for the two plans is shown in Fig. 12. DVHs for the MLCDAO and JODAO (15 aps) plan are plotted in Fig. 13. Note that in this case the jaws-only plan was not able to approach the dose conformity provided by the MLCDAO plan. It is likely that for large and irregularly shaped targets jaws-only IMRT will be unable to obtain high-quality plans using 20 or fewer apertures per beam direction. Therefore jaws-only IMRT may prove to lack the required delivery efficiency for these cases. The plan was delivered in approximately 13 min on an Elekta SL18 linear accelerator. The absolute dose measurement was 2.0% different from that predicted by the calculation. For comparison, the JODAO plan required 321 MU while the MLCDAO required 270 MU.

IV. SUMMARY AND CONCLUSION

Using direct aperture optimization, it is possible to create jaws-only IMRT treatment plans. The jaws-only approach can serve as a viable IMRT delivery technique for clinics without a multileaf collimator. The results demonstrate that in some cases jaws-only IMRT is able to produce similar plan quality to that provided with a traditional multileaf collimator based IMRT. In particular, jaws-only IMRT may prove useful for tangential breast IMRT and in prostate IMRT. For larger targets, complex target shapes, and cases involving multiple prescription levels, it is unlikely that a

jaws-only approach will be able to approach typical MLC-based IMRT plan quality. For the five cases included in this study an average treatment time of 18 min was observed. All five jaws-only delivery verifications provided absolute dose measurements that agreed within 5%.

ACKNOWLEDGMENTS

The authors would like to thank Prowess, Inc. for their support of this work. In particular, we would like to thank Mark Ping and John Nguyen.

^{a)}Electronic mail: mearl001@umaryland.edu

¹I. A. Baka, W. U. Laub, and F. Nusslin, "Compensators for IMRT—an investigation in quality assurance," *Z. Med. Phys.* **11**(1), 15–22 (2001).

²S. B. Jiang and K. M. Ayyangar, "On compensator design for photon beam intensity-modulated conformal therapy," *Med. Phys.* **25**(5), 668–675 (1998).

³K. Yoda and Y. Aoki, "A multiportal compensator system for IMRT delivery," *Med. Phys.* **30**(5), 880–886 (2003).

⁴J. R. Dai and Y. M. Hu, "Intensity-modulation radiotherapy using independent collimators: An algorithm study," *Med. Phys.* **26**(12), 2562–2570 (1999).

⁵S. Webb, "Fewer segments for IMRT generated by modulation splitting," *Phys. Med. Biol.* **47**(17), N217–222 (2002).

⁶S. Webb, "Intensity-modulated radiation therapy using only jaws and a mask: II. A simplified concept of relocatable single-bixel attenuators," *Phys. Med. Biol.* **47**(11), 1869–1879 (2002).

⁷S. Webb *et al.*, "Intensity-modulated radiation therapy using a variable-aperture collimator," *Phys. Med. Biol.* **48**(9), 1223–1238 (2003).

⁸M. A. Earl *et al.*, "Inverse planning for intensity-modulated arc therapy using direct aperture optimization," *Phys. Med. Biol.* **48**(8), 1075–1089 (2003).

⁹D. M. Shepard *et al.*, "Direct aperture optimization: A turnkey solution for step-and-shoot IMRT," *Med. Phys.* **29**(6), 1007–1018 (2002).

¹⁰S. Kirkpatrick, C. D. Gelatt, and M. P. Vecchi, "Optimization by simulated annealing," *Science* **220**, 671–680 (1993).